(2)

MECH-112

Contract N00014-86-K-0753, DARPA
Order No. 6065

INTERACTION OF PARTICULATE AND TRANSFORMATION TOUGHENING

John C. Amazigo and Bernard Budiansky

Division of Applied Sciences
HARVARD UNIVERSITY
Cambridge, Massachusetts 02138

December 1987

INTERACTION OF PARTICULATE AND TRANSFORMATION TOUGHENING

by

John C. Amazigo[1] and Bernard Budiansky
Division of Applied Sciences
Harvard University
Cambridge, MA 02138

ABSTRACT

A theoretical study is made of the interaction between the fracture toughening effects of crack-bridging ductile particles and phase-transforming particles embedded in a brittle matrix. It is found that in certain parametric ranges the interaction can be synergistic, with an increase in toughness produced that is greater than the sum of the increases that would be provided separately by the two types of reinforcement. Quantitative results are provided for the toughening in terms of the individual toughening effects and coupling parameters that depend on the properties of the uncoupled systems.

INTRODUCTION

The fracture toughness of ceramic materials can be increased through reinforcement by appropriately chosen ductile metal particles. A fairly general theoretical analysis of such *particulate toughening* in brittle-matrix composites, based on the assumption that the dominant mechanism is that of *crack bridging,* has been given by Budiansky, Amazigo, and Evans (1987). A different micromechanical toughening technique involves the incorporation of phase-transformable ceramic particles (notably ZrO_2) into the brittle matrix. The associated *transformation toughening* phenomenon, discovered by Garvie, Hannink, and Pascoe (1975), has been studied theoretically (McMeeking and Evans, 1982; Budiansky, Hutchinson, and Lambropoulos, 1983) on the presumption that the toughening is due to the crack-closing effects of dilatant phase transformations in the wakes of advancing cracks. It has been suggested (Evans, 1987) that

[1] On Sabbatical Leave from the Department of Mathematics, University of Nigeria, Nsukka, Nigeria.

(1)

ductile bridging particles and transforming particles might interact synergistically when they are both present, producing an increase in toughness greater than the sum of the effects they would provide separately.[2] The outcome of an elementary analysis by Budiansky (1986) indicated that the toughening ratio $\lambda = K/K_m$ (where K is the enhanced toughness and K_m is the toughness of the matrix) could sometimes be approximately equal to the product of the individual toughening ratios due to ductile particulates and transforming particles.

In this paper a theoretical study is made of the interacting effects of dilatant transforming particles and very ductile reinforcing particulates. The analysis will reveal conditions for the validity of the simple product rule for the toughening ratio, and will also provide quantitative results for the toughening ratio when these conditions are not met.

PARTICULATE TOUGHENING

The study by Budiansky, Amazigo, and Evans (1987) (denoted by BAE henceforth) contains the following result for the crack-bridging effect (Fig. 1) of ideally-plastic particles that obey the relation between particle stress σ_p and crack-face displacement v shown in Fig. 2. With K_p defined as the increased toughness in the presence of particles, the *modified* toughening ratio

$$\Lambda_p = \lambda_p/\sqrt{(1-c)} = \frac{K_p}{K_m\sqrt{1-c}} \tag{1}$$

is given by

$$\Lambda_p = \left[1 + \frac{2c}{1-c} \, \frac{ESv_f}{K_m^2(1-\nu^2)} \right]^{1/2} \tag{2}$$

where c is the volume concentration of particles, and, as shown in Fig. 2, S is the particle strength, and v_f is the displacement at fracture. The Young's modulus E and Poisson's ratio ν of the composite are assumed here, for simplicity, to be the same as those of the matrix material. This last simplification was not made in BAE, but is needed now to avoid undue complication later when transforming particles are introduced into the composite.

---

[2] Synergistic effects have evidently been observed (Becher and Tiegs, 1987) in ceramic composites toughened by a combination of *whiskers* and transforming particles.

An auxiliary formula in BAE provides a relation between Λ_P and the bridge length L_P at fracture:

$$\Lambda_P = 1 + \frac{cS}{K_m}\sqrt{\frac{8L_P}{\pi(1-c)}} \tag{3}$$

Eqs. (2) and (3) refer to the situation in which the bridged crack shown in Fig. 1 propagates in a steady-state fashion, with simultaneous occurrence of matrix cracking and failure of the particles at the end of the bridged zone.

TRANSFORMATION TOUGHENING

In the studies of transformation toughening by McMeeking and Evans (1982) and by Budiansky, Hutchinson, and Lambropoulos (1983) (hereafter denoted by BHL), it was assumed that during steady crack propagation martensitic-type transformations occur in particles when they are subjected to a critical mean stress σ_m^c. In the so-called supercritical case (discussed in detail in BHL) the full volumetric transformation strain θ_p^T is produced in each transforming particle in a zone A ahead of the crack tip as well as in its wake, as shown in Fig. 3. Along the curved front boundary C of this region, the mean stress σ_m^c is attained, and the dilatations thereby produced persist in a wake of height H_T on each side of the crack. With c_t defined as the volume concentration of transformable particles, which were assumed in BHL to have the same elastic moduli as the matrix, the key parameter governing transformation toughening emerges as

$$\omega = \frac{1+\nu}{1-\nu}\frac{Ec_t\theta_p^T}{\sigma_m^c} \tag{4}$$

Numerical results for the toughening ratio $\lambda_T = K_T/K_m$ were calculated by BHL for ω in the interval (0,20), and were extended by Amazigo and Budiansky (1987) to cover the full range of ω for which steady-state crack growth is possible. Fig. 4 shows $1/\lambda_T$ versus ω up to the critical "lock-up" value $\omega_c = 29.99$, first discovered by Rose (1986).

The zone size H_T is a function of ω in the form

$$\frac{H_T}{\left[(1+\nu)\dfrac{K_m}{\sigma_m^c}\right]^2} = g(\omega) \tag{5}$$

as shown in Fig. 5. The results of Figs. 4 and 5 combine to provide the alternative representation

$$\frac{H_T}{\left[(1+\nu)\dfrac{K}{\sigma_m^c}\right]^2} = f(\omega) \tag{6}$$

plotted in Fig. 6. As shown in BHL, the toughening is related to the zone size by

$$\lambda_T = [1+2\omega g(\omega)]^{1/2} \tag{7}$$

or, equivalently,

$$\lambda_T = [1-2\omega f(\omega)]^{-1/2} \tag{8}$$

Finally, we note that the toughening ratio can be expressed in terms of yet another zone-height parameter defined by

$$\frac{H_T}{\left[(1-\nu)\dfrac{K_m}{Ec_t\theta_p^T}\right]^2} = \omega^2 g(\omega) \tag{9}$$

For sufficiently small values of ω, the increase in toughness $\Delta K = K_T\text{-}K_m$ is given by

$$\Delta K = \left[\frac{E\sqrt{H_T}\,c_t\theta_p^T}{1-\nu}\right]\sqrt{g(0)} \tag{10}$$

where

$$g(0) = (4\pi\sqrt{3})^{-1} \tag{11}$$

COMBINED TOUGHENING EFFECTS

The results for particulate and transformation toughening are deficient in various ways. A few available measurements for particulate toughening versus bridge length (BAE) are consistent with Eq.(3) only if questionably high values of particle strength S are presumed. Transformation-toughening data collected by Evans and Cannon(1986) show that the increase in toughness appears to be proportional to $\sqrt{H_T}$, but the experimental values of ΔK are substantially greater than those predicted by Eq.(10). Current thinking (Evans,1987) points to the likelihood that shear stress may play a role at least as important as mean stress in triggering the phase transformation. We nevertheless pursue the theoretical analysis of the interaction of particulate and transformation toughening on the basis of the present models, with the hope that final results will be useful when they are interpreted in terms of *experimental* input values of Λ_P and λ_T.

The analysis in Appendix A provides results for the combined *modified* toughening ratio

$$\Lambda = \frac{K}{K_m\sqrt{1-c}} \tag{12}$$

in terms of Λ_P, λ_T, and a coupling parameter

$$\rho = \frac{(1+\nu)cS}{\sigma_m^c} \tag{13}$$

that governs the interaction between particulate and transformation toughening when they occur simultaneously during steady crack growth (Fig. 7). Representative numerical results are shown in Figs. 8-10 for Λ versus λ_T, for Λ_P = 2,3,4, respectively. The individual curves in each figure are for selected values of the coupling parameter in the range $[0,\infty]$.

The limiting results for $\rho=\infty$ and 0 are of special interest. As explained in Appendix B, we have

$$\Lambda = \Lambda_P\lambda_T \qquad \text{for } \rho \to \infty \tag{14}$$

and

$$\Lambda = [\,\Lambda_P^2 + \lambda_T^2 - 1]^{1/2} \qquad \text{for } \rho \to 0 \tag{15}$$

Thus the previously anticipated product rule $\lambda = \lambda_P\lambda_T$ for the combined toughening ratio holds in the first limiting case. In this limit, as well as for sufficiently large finite values of ρ, transforming and bridging particles interact synergistically, producing a larger increase in toughness than the sum of the increases that would occur separately. On the other hand, for ρ approaching zero, the combined increase can be substantially less than cumulative.

Unfortunately, in view of the uncertainties mentioned concerning the bases for the analysis, an appropriate choice for the coupling parameter ρ is not easily made. However, the results of the analysis can be recast in terms of an alternative coupling parameter that is much more illuminating. In terms of the zone height H_T for pure transformation toughening, and the bridge length L_P for pure particulate toughening, the new coupling parameter is defined as

$$\eta = \frac{H_T(1-c)}{L_P} \tag{16}$$

The counterparts to Figs. 8-10 are shown in Figs. 11-13, with curves showing Λ for various values of η. An appropriate choice for η can now be made on the basis of *observations* of the separate toughening phenomena, bypassing the need to estimate dubious parameters in the underlying theory.

It is striking that quite small values of η suffice to provide results close to those for $\eta = \rho = \infty$, for which the synergistic product rule applies. This is a happy result, because it means that synergism is not precluded despite the fact that transformation-toughening zone heights tend to be smaller than particulate bridge lengths.

At fracture, the actual transformation-zone size H and bridge length L (Fig. 7) are generally different from their uncoupled values H_T and L_P. It turns out (Appendix C) that H satisfies

$$\frac{H}{H_T(1-c)} = \frac{\Lambda^2 - \Lambda_P^2}{\lambda_T^2 - 1} \tag{17}$$

Hence, for given values of Λ_P and λ_T, the quantity $H/[H_T(1-c)]$ is an increasing function of the coupling parameter, with (see Eqs.(14,15))

$$\frac{H}{H_T(1-c)} = 1 \qquad \text{for } \eta = 0$$

$$= \Lambda_P^2 \quad \text{for } \eta = \infty$$

Fig. 14 illustrates how $H/[H_T(1-c)]$ varies with η for the case $\Lambda_P=2$ and $\lambda_T=3$.

A simple general formula for L/L_P is not available, but numerical results for L/L_P vs. η, again for $\Lambda_P = 2$, $\lambda_T = 3$, are shown in Fig. 15. It is shown in Appendix C that L/L_P increases from

$$\frac{L}{L_P} = \left[\frac{(\Lambda_P^2 + \lambda_T^2 - 1)^{1/2} - \lambda_T}{\Lambda_P - 1} \right]^2 \tag{18}$$

at $\eta = 0$ to $L/L_P = 1$ for $\eta \to \infty$.

The essence of the interactive process is the increase in transformation-zone height at fracture that is produced by the presence of bridging particles. At maximum synergism, for which the product rule applies, the zone height is amplified by the factor λ_P^2.

CONCLUDING REMARKS

The possibility of synergism between particulate and transformation toughening has been demonstrated on the basis of simple models for the individual toughening processes and their interaction. The essential requirement for synergistic interaction is that in the uncoupled situations the transformation zone size not be too small relative to the particulate bridging length. However, this requirement is not severe; ratios of zone height to bridge length of 1/10, or even less, may suffice to provide synergistic effects.

It would be desirable to corroborate these conclusions by repeating the analysis on the basis of more realistic assumptions concerning ductile-particle constitutive behavior and criteria for phase tranformation.

ACKNOWLEDGEMENTS

This work was supported by DARPA University Research Initiative (Subagreement P. O. #VB38639-0 with the University of California, Santa Barbara, ONR Prime Contract N00014-86-K-0753), the Office of Naval Research (Contract N00014-84-K-0510), the National Science Foundation (Grant MSM-84-16392), and the Division of Applied Sciences, Harvard University.

REFERENCES

AMAZIGO, J. C., and BUDIANSKY, B. 1987 "Steady-State Crack Growth in Subcritically Transforming Materials", Harvard University Report MECH-107 (to be published in *Int. J. Solids Structures*)

BECHER, D. F., and TIEGS, T. N. 1987 *J. Am. Ceram. Soc.*, **70**, pp. 651-654

BUDIANSKY, B. 1986 "Micromechanics II", *Proceedings of the Tenth U. S. National Congress of Applied Mechanics*, Austin, Texas, June 16-20, 1986

BUDIANSKY, B., AMAZIGO, J. C., and EVANS, A. G. 1987 "Small -Scale Crack Bridging and the Fracture Toughness of Particulate-Reinforced Ceramics", Harvard University Report MECH-104 (to be published in *J. Mech. Phys. Solids*)

BUDIANSKY, B., HUTCHINSON, J. W. and LAMBROPOULOS, J. C. 1983 *Int. J. Solids Structures*, **19**, pp. 337-355

EVANS, A. G. 1987 "The New High Toughness Ceramics" (to be published by ASTM)

GARVIE, R. C., HANNINK, R. H., and PASCOE, R. T. 1975 *Nature*, **258**, pp. 703-704.

McMEEKING, R. M., and EVANS, A. G. 1983 *J. Am. Ceram. Soc.*, **65**, pp. 242-246

APPENDIX A

INTERACTION ANALYSIS

We contemplate a steadily growing semi-infinite crack (Fig. 7) subjected far from the crack tip to conventional K-field stresses

$$\sigma_{\alpha\beta} = \frac{K}{\sqrt{2\pi R}} f_{\alpha\beta}(\phi) \qquad (f_{22}(0) = 1) \tag{A1}$$

corresponding to the standard Muskhelishvili potential

$$\phi_K = \frac{K}{\sqrt{2\pi}}\sqrt{Z} \tag{A2}$$

The crack is constrained by bridging particles over a length L, and, as in BHL, uniformly distributed plane-strain dilatation of magnitude

$$\Omega = \frac{2}{3}(1+\nu)c_t\theta_p^T \tag{A3}$$

is assumed to occur in the shaded region A. It can be shown that the elastic field associated with the smeared-out crack-face tensions cS supplied by the bridging particles is characterized by a Muskhelishvili potential ϕ_P satisfying

$$\frac{\partial\phi_P(Z)}{\partial Z} = \frac{cS}{\pi}\left[-\sqrt{\frac{L}{Z}} + \frac{i}{2}\log\left(\frac{\sqrt{Z}-i\sqrt{L}}{\sqrt{Z+i\sqrt{L}}}\right)\right] \tag{A4}$$

and the field due to the transforming particles is described by

$$\phi_T = \frac{E\Omega}{4\pi(1-\nu^2)}\int_C \log[(Z^{1/2} + Z_0^{1/2})(Z^{1/2} + \bar{Z}_0^{1/2})]dY_0 \tag{A5}$$

outside the transformed region. The integral is along the curved front boundary C of the transformed region. Substitution of the total potential

$\phi = \phi_K + \phi_P + \phi_T$ into the jump relation

$$v^+(X) = \frac{2(1-\nu^2)}{iE}[\phi(X)]_-^+ \tag{A6}$$

gives the displacement of the upper crack-face along $X < 0$, and the mean stress outside A is given by

$$\sigma_m = \frac{4(1+\nu)}{3} \mathrm{Re}\left(\frac{\partial\phi}{\partial Z}\right) \tag{A7}$$

During steady crack growth, the displacement at $X = -L$ remains equal to its failure value v_f, and the transformation criterion $\sigma_m = \sigma_m^c$ must be met as Z approaches C from the exterior of A. Assertion of these two conditions provides the relations

$$v_f = \frac{4(1-\nu^2)K\sqrt{L}}{E\sqrt{2\pi}} - \frac{4cS(1-\nu^2)L}{\pi E} - \frac{2(1+\nu)c_t\theta_p^T}{3\pi} \mathrm{Im} \int_C \log\left[\frac{\sqrt{Z_0}+i\sqrt{L}}{\sqrt{Z_0}-i\sqrt{L}}\right] dY_0 \tag{A8}$$

and

$$\sigma_m^c = \frac{2K(1+\nu)}{3} \mathrm{Re}\left(\frac{1}{\sqrt{2\pi Z}}\right) - \frac{2(1+\nu)cS}{3\pi}\left[2\mathrm{Re}\sqrt{\frac{L}{Z}} + \mathrm{Im}\left(\log\frac{\sqrt{Z}-i\sqrt{L}}{\sqrt{Z}+i\sqrt{L}}\right)\right]$$

$$-\left(\frac{1+\nu}{1-\nu}\right)\frac{Ec_t\theta_p^T}{9\pi} \mathrm{Re}\left[\frac{1}{\sqrt{Z}}\int_C\left(\frac{1}{Z^{1/2}+Z_0^{1/2}} + \frac{1}{Z^{1/2}+\bar{Z}_0^{1/2}}\right)dY_0\right] \tag{A9}$$

The I-integral of BHL, modified to account for the presence of the ductile particles, gives

$$\frac{K^2(1-\nu^2)}{E} = \frac{K_m^2(1-\nu^2)(1-c)}{E} + 2cSv_f + 2H\sigma_m^c c_t\theta_p^T \tag{A10}$$

and another connection between K and K_m that follows directly from a combination of relations in BAE and BHL is

$$K_m\sqrt{1-c} = K - cS\sqrt{\frac{8L}{\pi}} - \frac{Ec_t\theta_p^T}{3(1-\nu)}\sqrt{\frac{2}{\pi}} \mathrm{Re}\int_C \frac{dY}{\sqrt{Z}} \tag{A11}$$

With the introduction of the non-dimensional variables $w = v/D$, $z = x+iy = re^{i\phi} = Z/D$, $l = L/D$, and $h = H/D$ in terms of the characteristic distance

$$D = \frac{2(1-c)}{9\pi}\left[\frac{(1+\nu)K_m}{\sigma_m^c}\right]^2 \tag{A12}$$

the governing equations (A8-A11) become

$$w_f = \Lambda\sqrt{l} - \frac{2\rho l}{3\pi} - \frac{\omega}{9\pi}\,\mathrm{Im}\int_C \log\left[\frac{1+i\sqrt{\frac{l}{z}}}{1-i\sqrt{\frac{l}{z}}}\right]dy \qquad \text{(A13)}$$

$$\Lambda\,\mathrm{Re}\left(\frac{1}{\sqrt{z}}\right) - \frac{2\rho}{3\pi}\left[2\mathrm{Re}\left(\sqrt{\frac{l}{z}}\right) + \mathrm{Im}\log\left(\frac{1-i\sqrt{\frac{l}{z}}}{1+i\sqrt{\frac{l}{z}}}\right)\right]$$

$$-\frac{\omega}{9\pi}\,\mathrm{Re}\left[\frac{1}{\sqrt{z}}\int_C\left(\frac{1}{z^{1/2}+z_0^{1/2}}+\frac{1}{z^{1/2}+\bar{z}_0^{1/2}}\right)dy_0\right] = 1 \qquad \text{(A14)}$$

$$\Lambda^2 = 1 + \frac{4}{3\pi}\left(2\rho w_f + \frac{\omega h}{3}\right) \qquad \text{(A15)}$$

$$\Lambda = 1 + \frac{4\rho\sqrt{l}}{3\pi} + \frac{2\omega}{9\pi}\,\mathrm{Re}\int_C \frac{dy}{\sqrt{z}} \qquad \text{(A16)}$$

where ω, Λ, and ρ are defined in Eqs. (4), (12), and (13).

For prescribed values of Λ_P, λ_T, and ρ, the solution for Λ was found as follows. The value of ω is known as a function of λ_T (Fig. 4), and w_f may be found from the relation

$$\Lambda_P^2 = 1 + \frac{8\rho w_f}{3\pi} \qquad \text{(A17)}$$

given by (A16) for $\omega = 0$ (which gives Eq.(2) of the text). The boundary C in the z-plane was represented by $r(\phi)$ in the interval $(-\phi_m, \phi_m)$ and the expansion

$$r(\phi)\sin(\phi) = \sum_{n=1}^{N} b_n \sin\left[(n-1/2)\frac{\pi\phi}{\phi_m}\right] \qquad \text{(A18)}$$

was assumed. The N+3 unknowns b_n (n=1,2,..N), ϕ_m , l , and Λ were found by solving simultaneously Eq. (A13), (A16), and the assertion of Eq. (A14) at $\phi_j=(j\phi_m/N)$, j=0,1,2,...N.

With $h = r(\phi_m)\sin(\phi_m)$, Eq. (A15) provided a check on the value of Λ. Only a few b_n's were needed for adequate accuracy in the preparation of Figs. (8-10).

The alternative coupling parameter η (Eq. 16) is given in terms of ρ by the formula

$$\eta = \frac{4\rho^2}{\pi\omega}\,\frac{\lambda_T^2 - 1}{(\Lambda_P - 1)^2} \tag{A19}$$

that follows from Eqs. (3), (5), (7) and (13).

APPENDIX B

LIMITING VALUES OF TOUGHENING RATIO

For $\rho \to \infty$ but Λ_P fixed, we can imagine $S \to \infty$, $L \to 0$, with $S\sqrt{L}$ and Sv_f bounded. It can be verified that in this limit the potential ϕ_P defined by Eq. (A4) vanishes for all $Z \neq 0$, but as shown by Eq. (A11), the crack-face stresses nevertheless continue to affect the crack-tip stress-intensity factor $K_{tip} = K_m(1-c)^{1/2}$. Perform the following thought experiment: in the absence of bridging particles, apply K, and let the phase transformations occur. The zone height $H = H_T$ will be given by Eq. (6). Now introduce the particles, and note that since the stresses do not change for $Z \neq 0$, neither will H; hence Eqs. (A10), (2), and (6) give

$$\frac{K^2(1-\nu^2)}{E} = \frac{K_m^2(1-\nu^2)\Lambda_P^2(1-c)}{E} + \frac{2\omega f(\omega) K^2(1-\nu^2)}{E}$$

It follows, via (8), that $\Lambda^2/(\lambda_T)^2 = (\Lambda_P)^2$, and so $\lambda = \lambda_P \lambda_T$.

Next, for the case $\rho \to 0$, we pretend that $S \to 0$, $L \to \infty$, again keeping $S\sqrt{L}$ bounded. In this limit, the particle potential prescribed by Eq. (A4) becomes indistinguishable from one due to a K-field (Eq.(A2)). Withholding the ductile particles, apply K, and adjust its value to make $K_{tip} = K_m(1-c)^{1/2}$. By (5), the transformation-zone height will assume the magnitude

$$H = g(\omega)\left[\frac{(1+\nu)K_m}{\sigma_m^c}\right]^2 (1-c)$$

Next, introduce the bridging particles, and add an equivalent increment to K to keep H unchanged. The total K will now satisfy the relation

$$\frac{K^2(1-\nu^2)}{E} = \frac{K_m^2(1-\nu^2)\Lambda_P^2(1-c)}{E} + \frac{2\omega g(\omega) K_m^2(1-\nu^2)(1-c)}{E}$$

that follows from (A10), and then (7) gives $\Lambda^2 = (\Lambda_P)^2 + (\lambda_T)^2 - 1$.

APPENDIX C

TRANSFORMATION-ZONE HEIGHT AND BRIDGE LENGTH

From Eqs. (5), (7), and the definition (A12) for D, we have

$$\frac{H_T}{D} = \frac{9\pi}{4(1-c)}\left[\frac{\lambda_T^2-1}{\omega}\right] \tag{C1}$$

Using h = H/D in Eq. (A15), together with Eq. (A17) gives

$$\frac{H}{D} = \frac{9\pi}{4\omega}(\Lambda^2-\Lambda_P^2) \tag{C2}$$

and combining (C1) and (C2) provides the result (17).

To calculate L/L_P from the results of the numerical procedure of Appendix A, we write

$$\frac{L}{L_P} = \frac{L}{H}\,\frac{H}{H_T(1-c)}\,\frac{H_T(1-c)}{L_P}$$

Using Eqs. (16-17) gives the formula

$$\frac{L}{L_P} = \frac{\eta l}{h}\left(\frac{\Lambda^2-\Lambda_P^2}{\lambda_T^2-1}\right) \tag{C3}$$

that was used to prepare Fig. 15.

The limiting values of L/L_P follow from the observation that setting $\omega = 0$ in (A16) (or using (3)) gives

$$\Lambda_P = 1 + \frac{4\rho\sqrt{l_P}}{3\pi} \tag{C4}$$

Combining this with Eq. (A16) gives the general result

$$\frac{l}{l_P} = \frac{L}{L_P} = \left[\frac{\Lambda-1-\frac{2\omega}{9\pi}\,\mathrm{Re}\int_c \frac{dy}{\sqrt{z}}}{\lambda_P-1}\right]^2 \tag{C5}$$

But now recall the argument in Appendix B for the limiting case $\rho \to 0$, wherein field stresses were unaffected by the introduction of particles and the simultaneous increase of K. This implies that for $\rho \to 0$ the integral in (C5) keeps the same non-dimensional value it would have had in the case of pure transformation toughening. Hence, for $\rho \to 0$. and

$$\lambda_T = 1 + \frac{2\omega}{9\pi} \operatorname{Re} \int_C \frac{dz}{\sqrt{z}}$$

we get

$$\frac{L}{L_P} = \left(\frac{\Lambda - \lambda_T}{\Lambda_P - 1}\right)^2$$

which gives (18).

For $\rho \to \infty$, on the other hand, the argument in Appendix B had the transformation zone unchanged with K *fixed* when particles were introduced. Hence, in this case, the integral in (C5) is Λ/λ_T times the value for transformation toughening. Accordingly,

$$\frac{L}{L_P} = \left[\frac{\Lambda - 1 - \frac{\Lambda}{\lambda_T}(\lambda_T - 1)}{\Lambda_P - 1}\right]^2$$

and the limit $\Lambda = \Lambda_P \lambda_T$ for $\rho \to \infty$ gives $L/L_P = 1$.

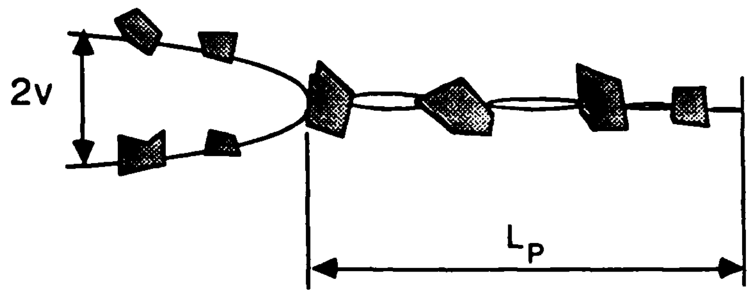

Fig. 1 Bridged crack.

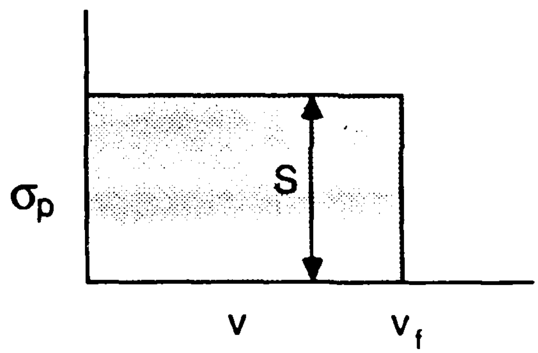

Fig. 2 Particle stress versus crack-face displacement.

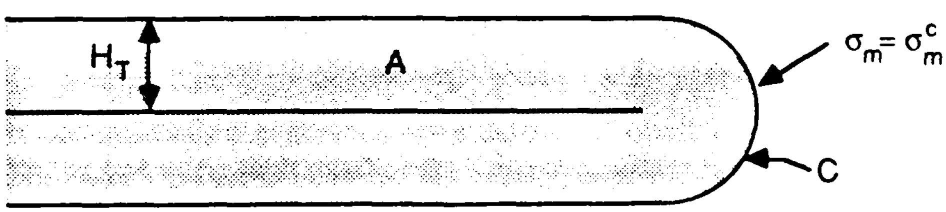

Fig. 3 Zone of phase-transformed particles.

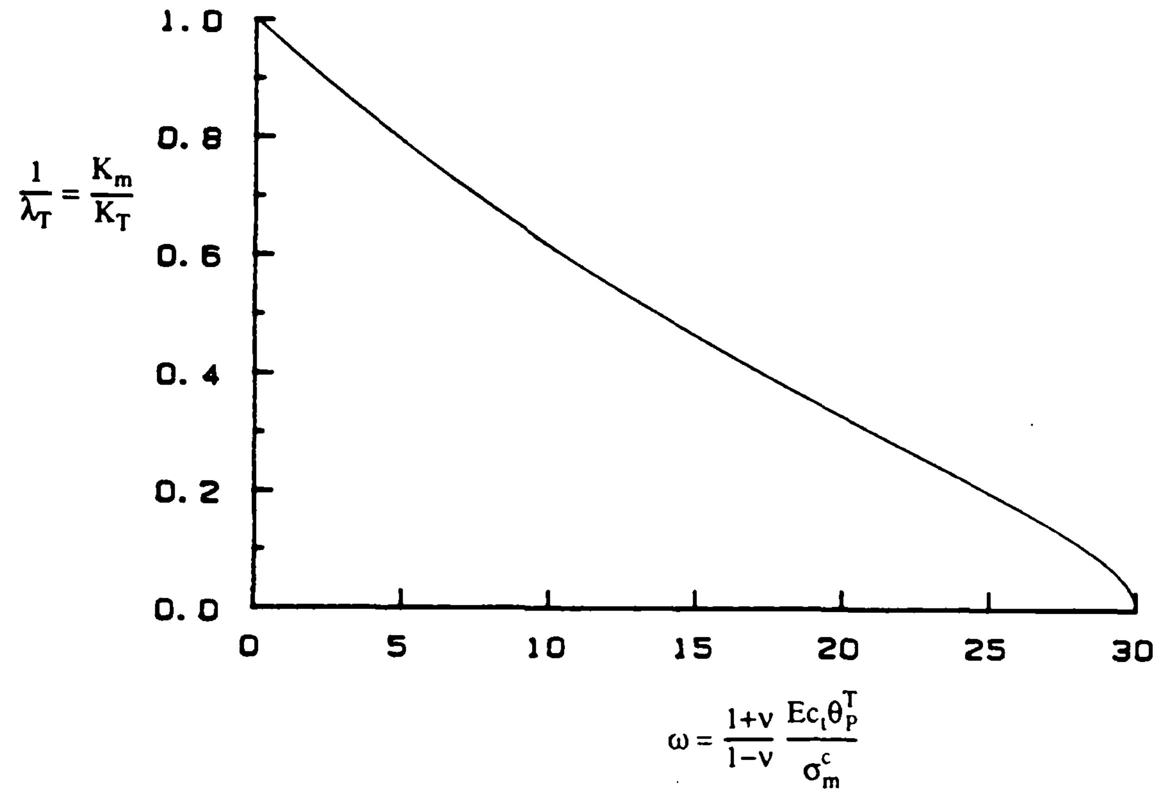

Fig. 4 Transformation toughening: reciprocal of toughening ratio versus toughening parameter, up to "lock-up".

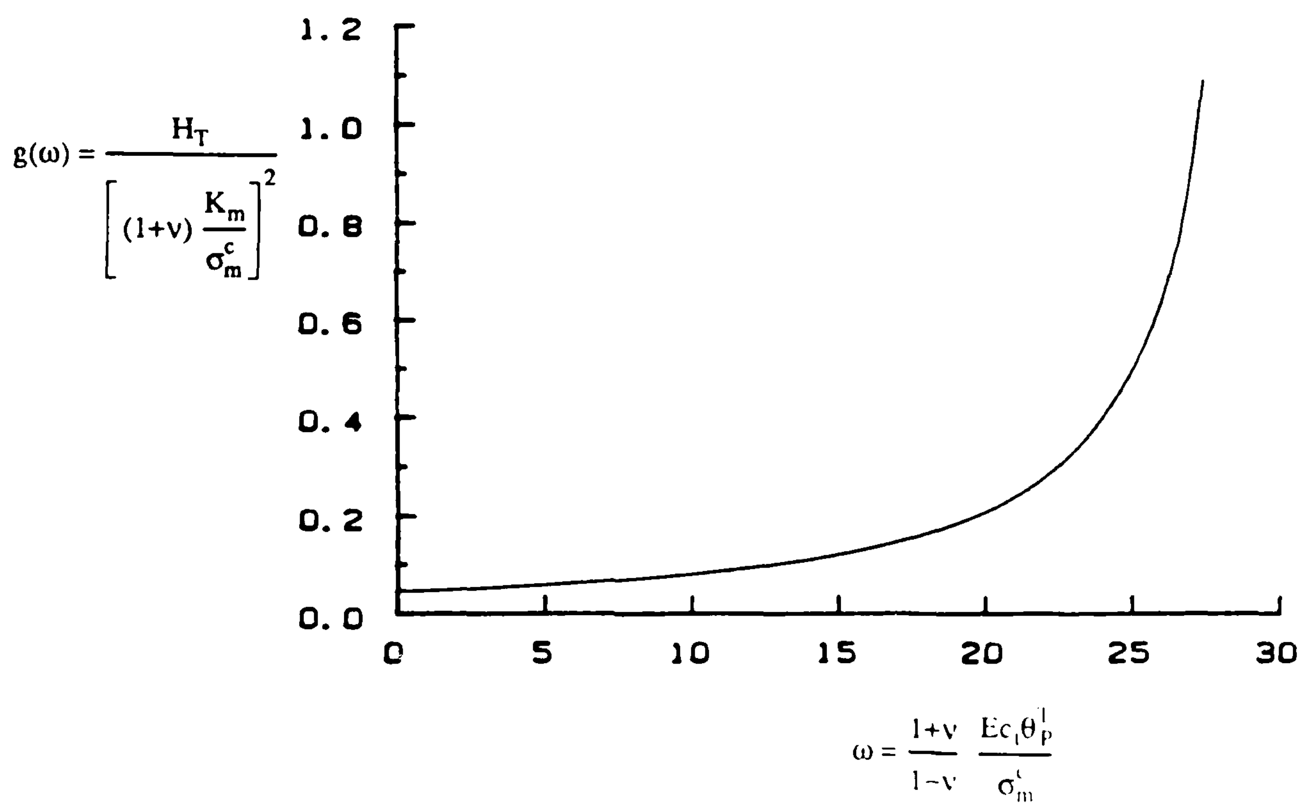

Fig. 5 Dependence of transformation zone-height on toughening parameter.

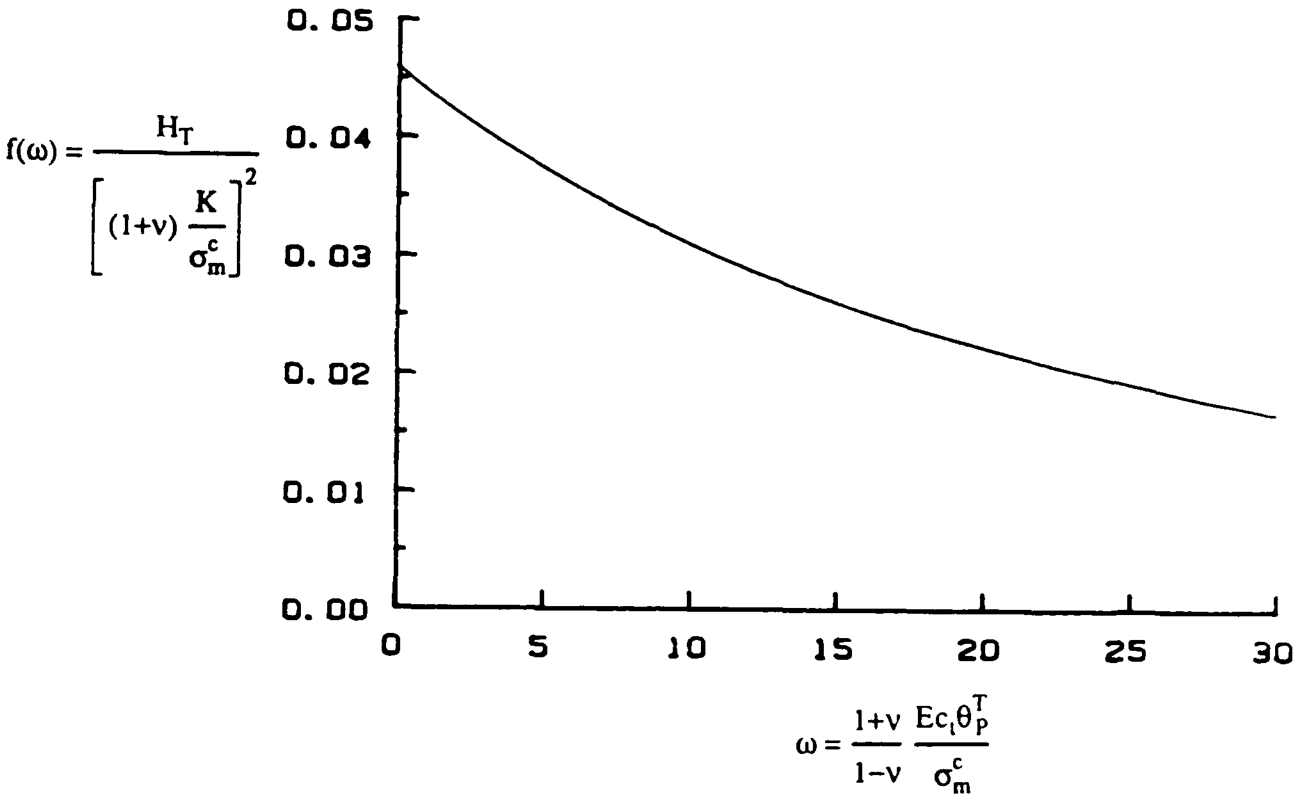

Fig. 6 Dependence of transformation zone-height on toughening parameter.

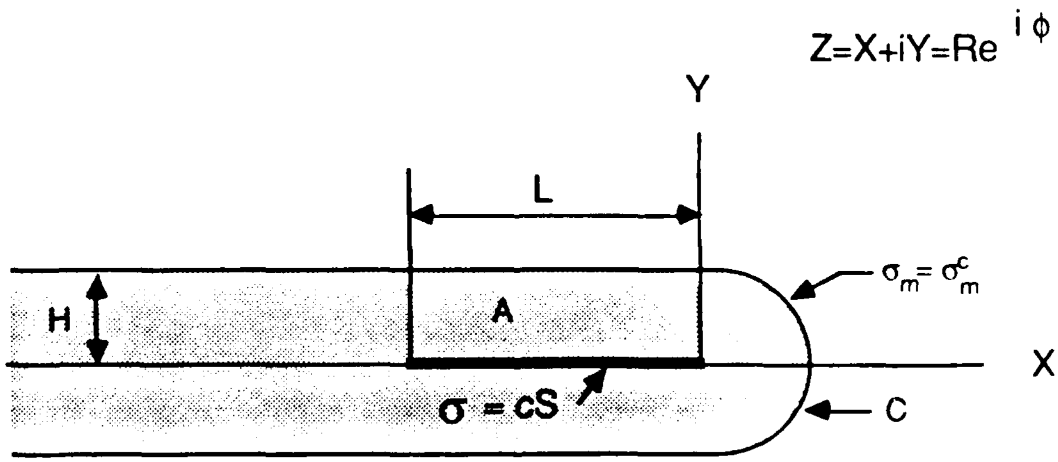

Fig. 7 Bridged length and transformed zone during steady crack growth.

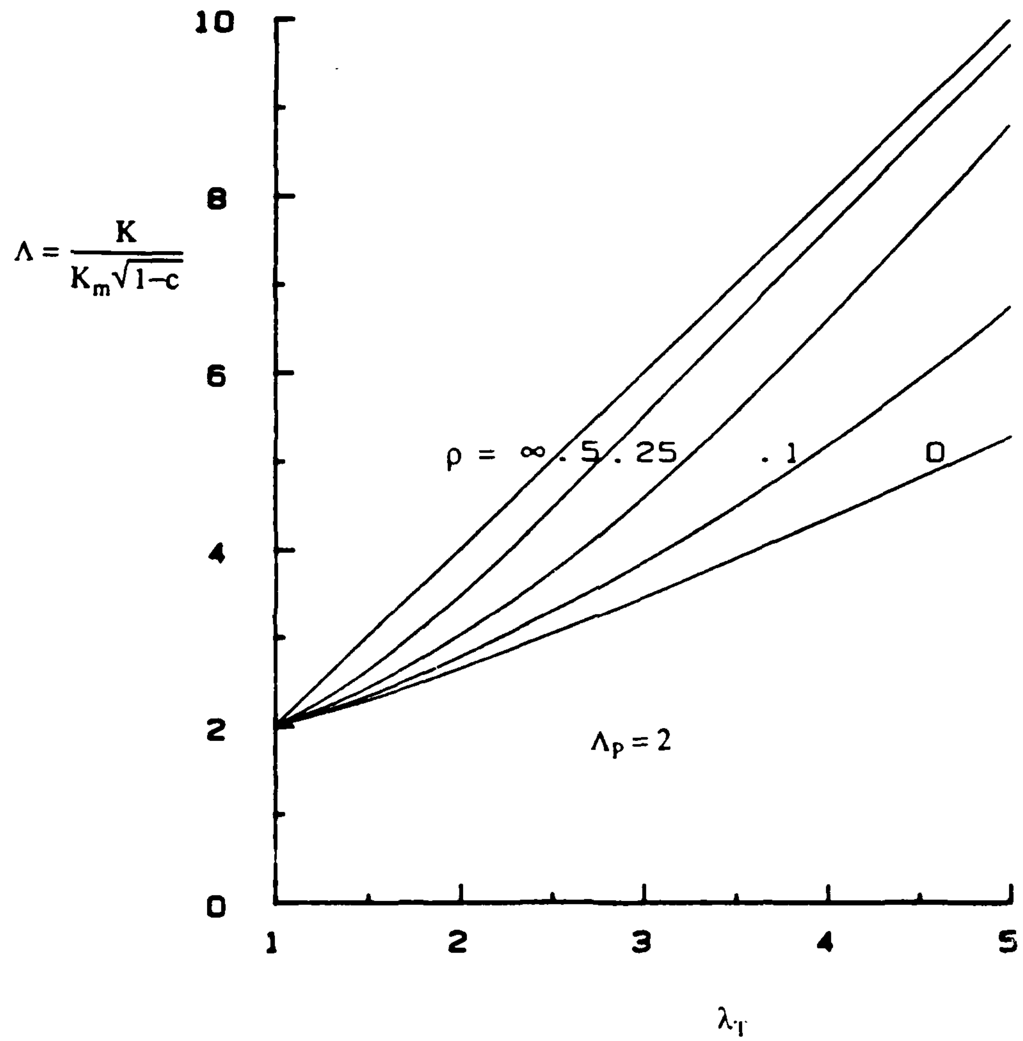

Fig. 8 Modified toughening ratio for various values of coupling parameter $\rho = (1+\nu)cS/\sigma_m^c$; $\Lambda_P = 2$.

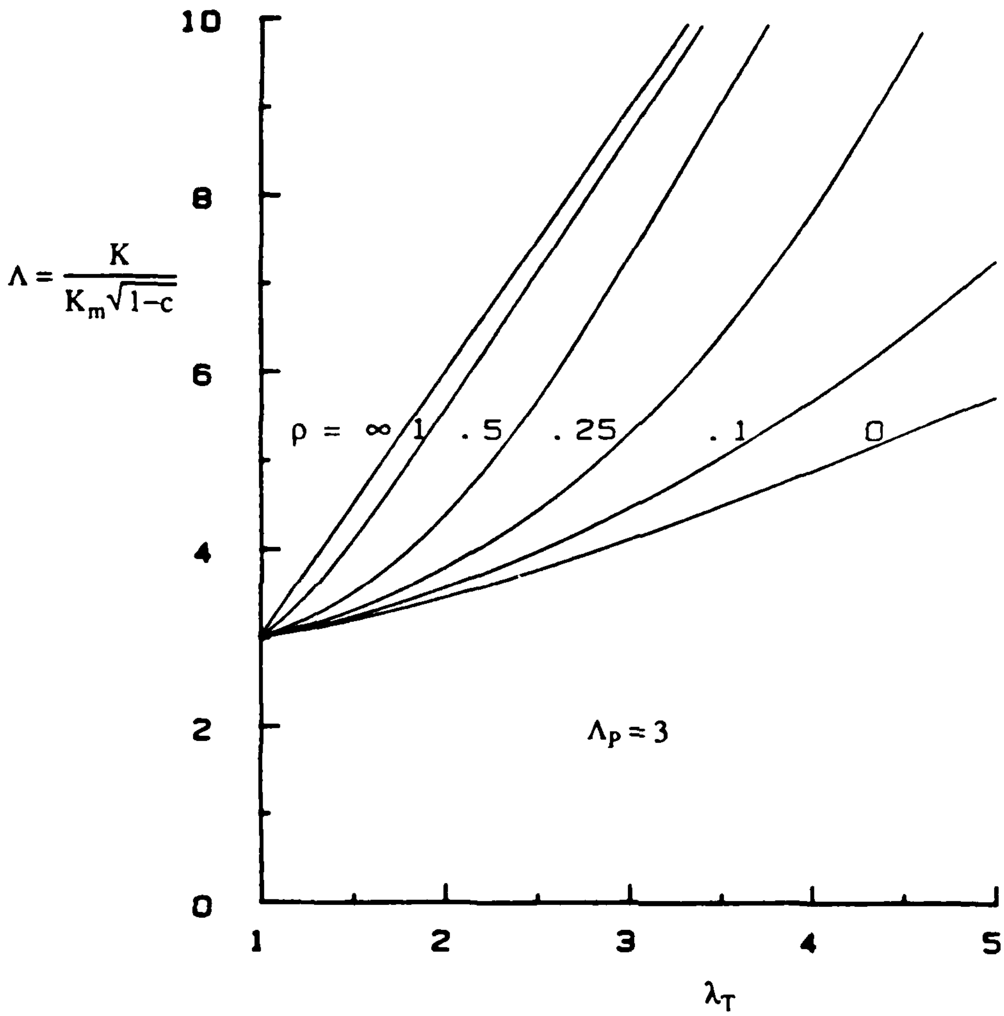

Fig. 9 Modified toughening ratio for various values of coupling parameter $\rho = (1+\nu)cS/\sigma_m^c$; $\Lambda_P = 3$.

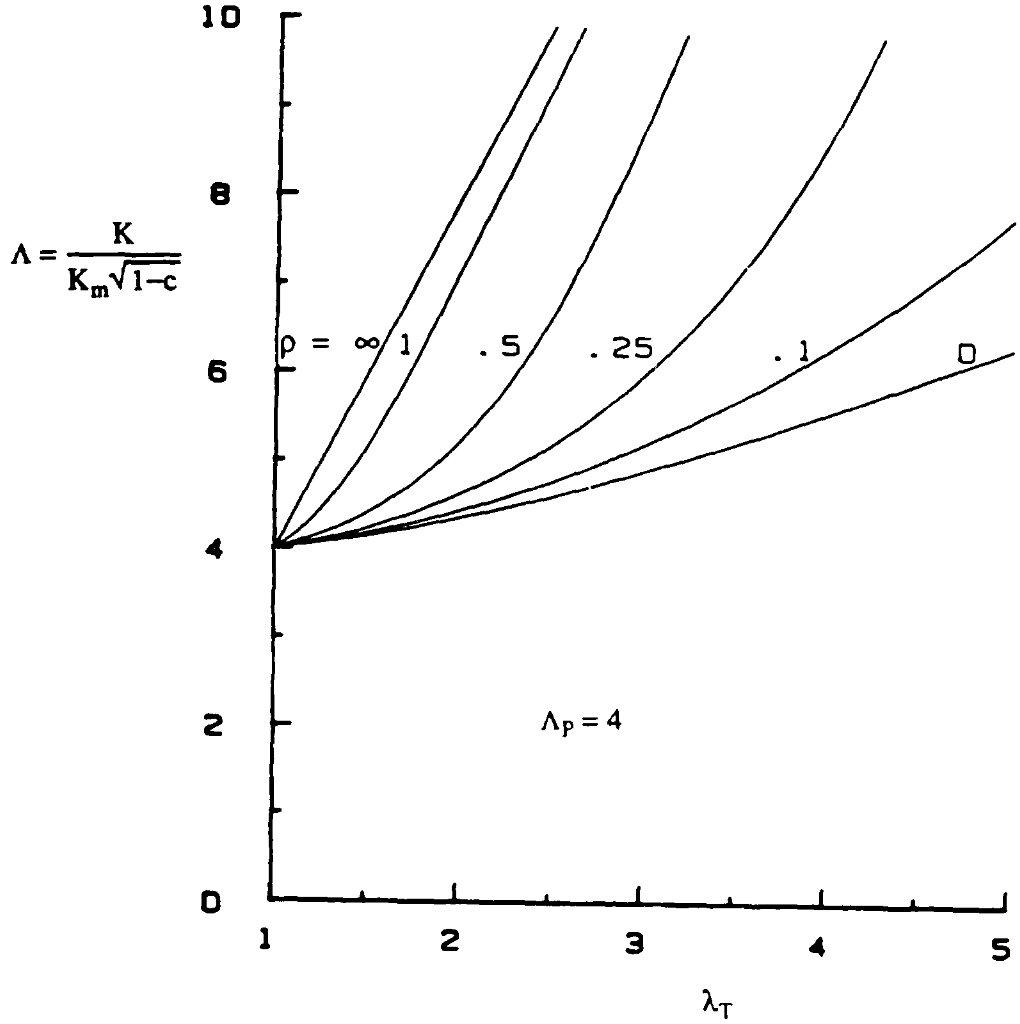

Fig. 10 Modified toughening ratio for various values of coupling parameter $\rho = (1+\nu)cS/\sigma_m^c$; $\Lambda_P = 4$.

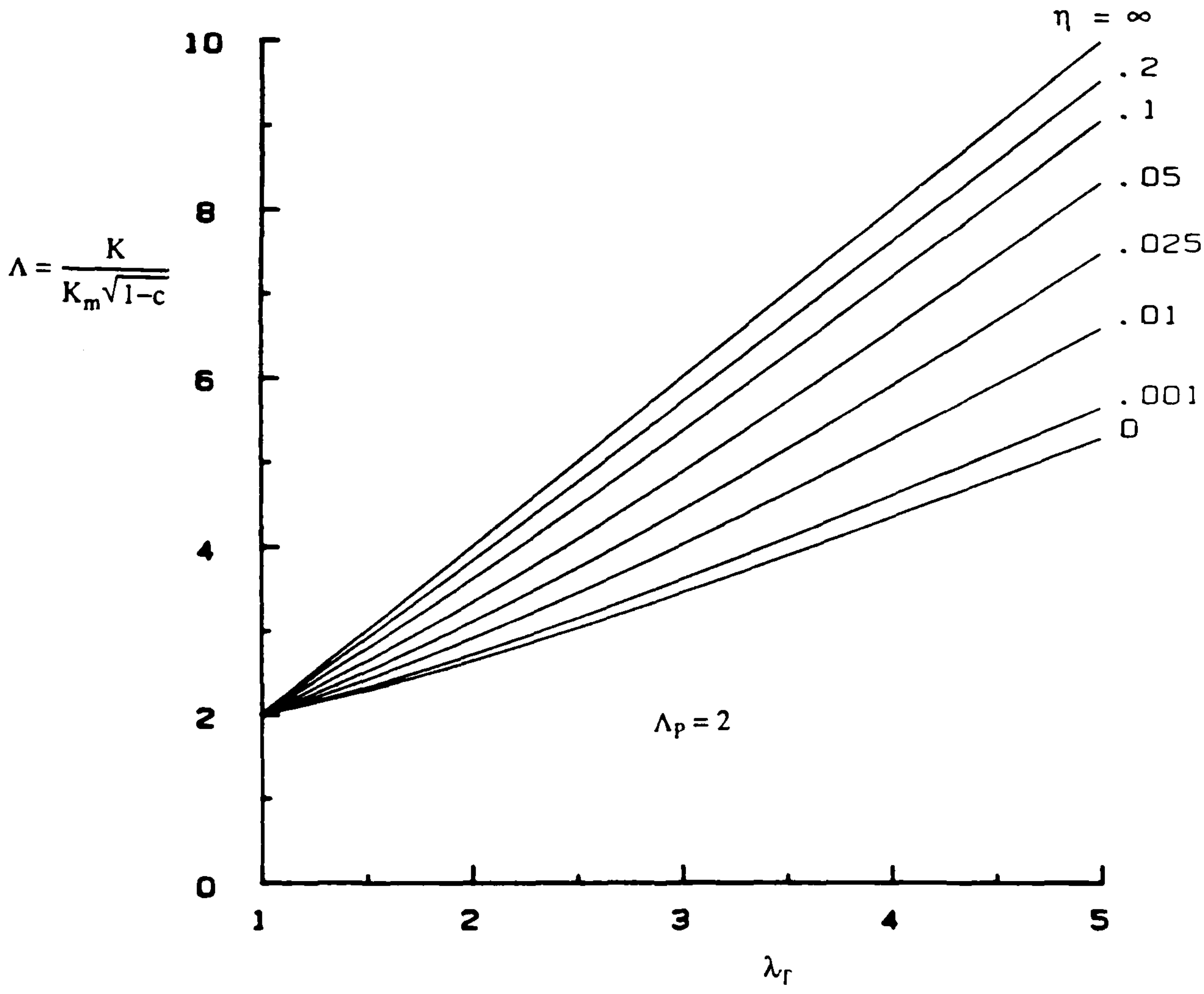

Fig. 11 Modified toughening ratio for various values of coupling parameter $\eta = H_T(1-c)/L_P$; $\Lambda_P = 2$.

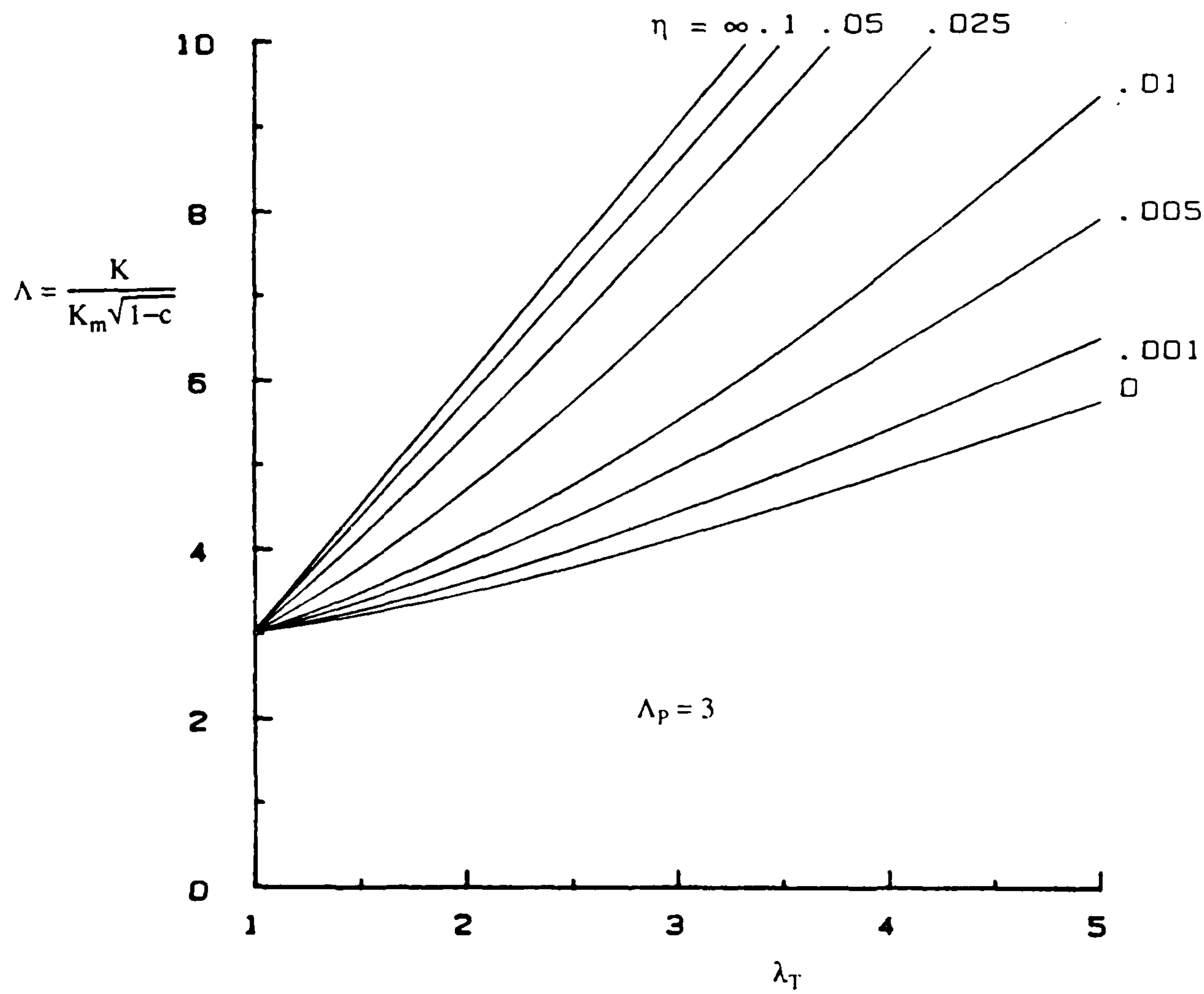

Fig. 12 Modified toughening ratio for various values of coupling parameter $\eta = H_T(1-c)/L_P$; $\Lambda_P = 3$.

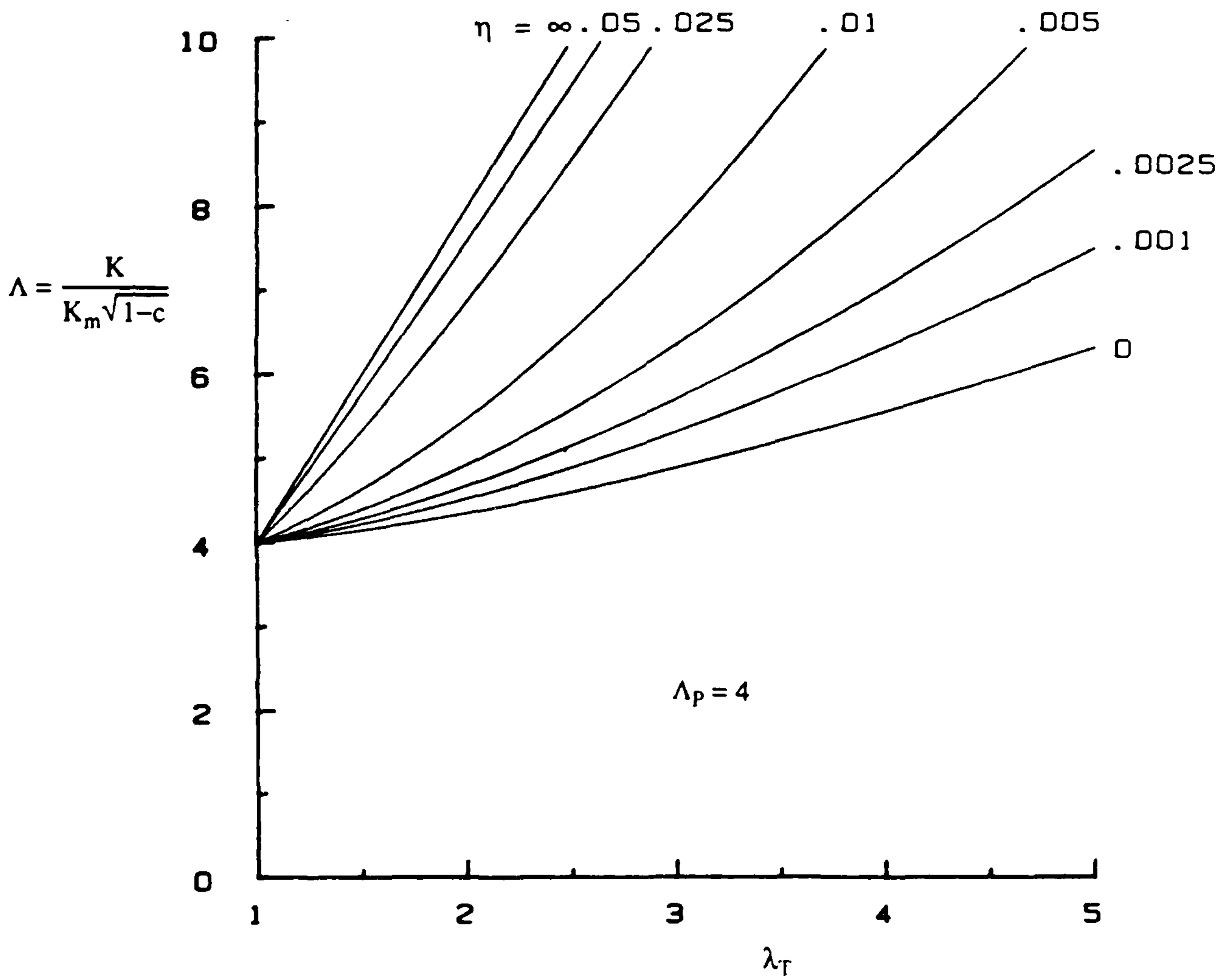

Fig. 13 Modified toughening ratio for various values of coupling parameter $\eta = H_T(1\text{-}c)/L_P$; $\Lambda_P = 4$.

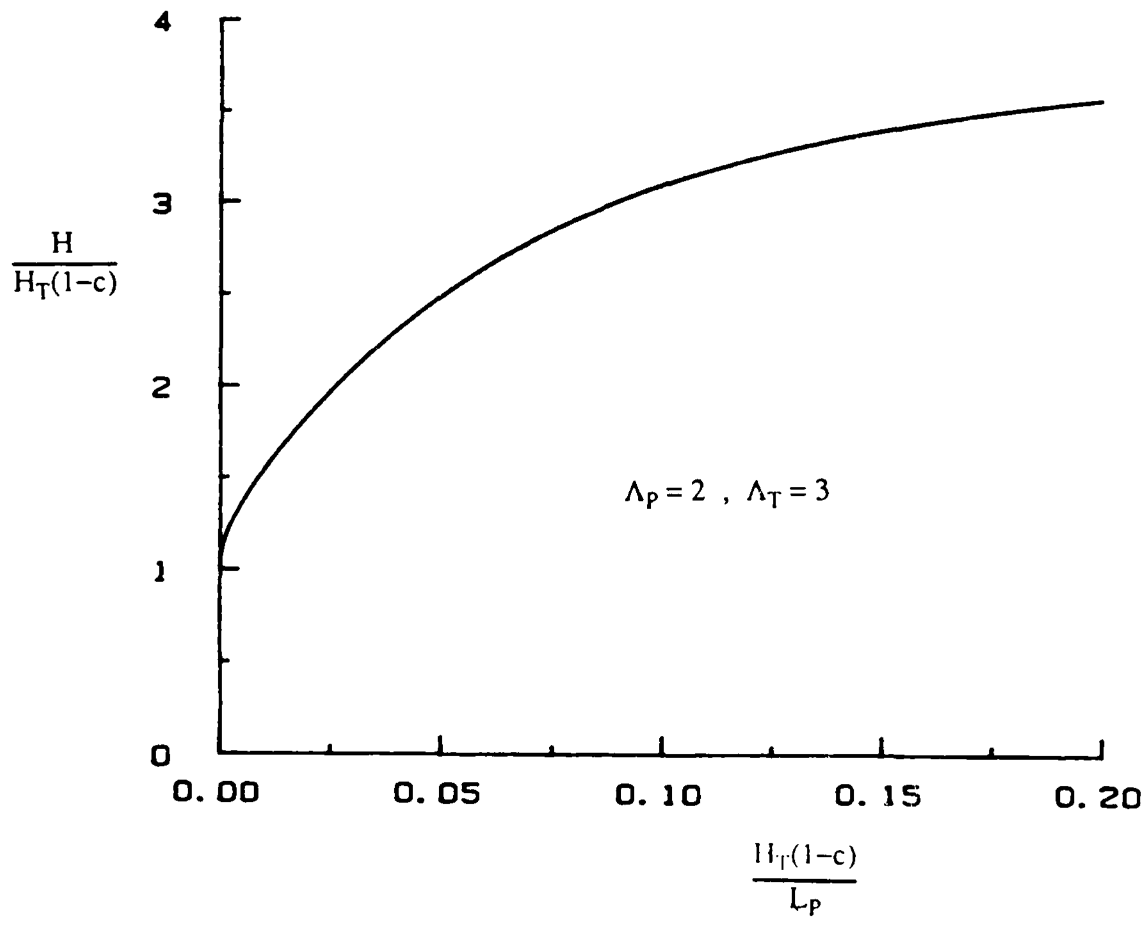

Fig. 14 Dependence of transformed-zone height on coupling parameter $\eta = H_T(1\text{-}c)/L_P$; $\Lambda_P = 2$, $\Lambda_P = 3$.

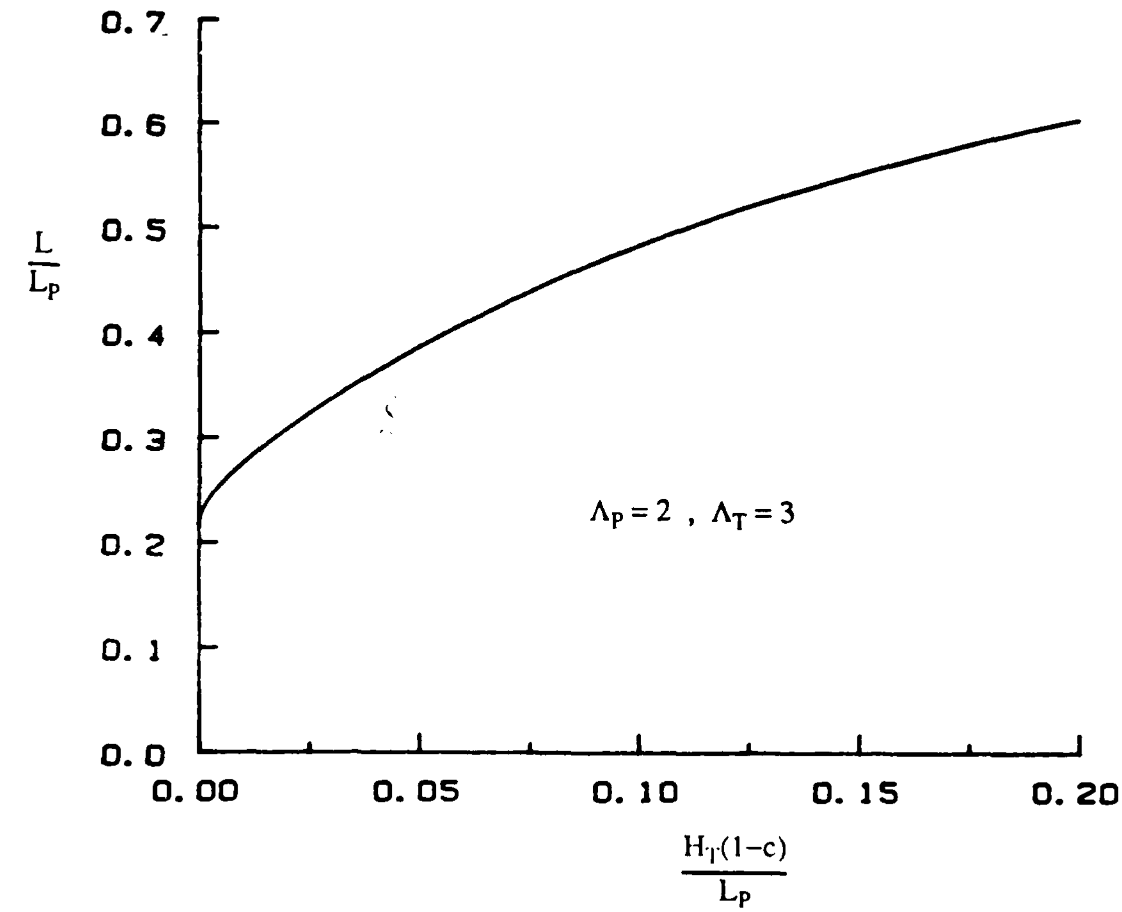

Fig. 15 Dependence of bridge length on coupling parameter $\eta = H_T(1\text{-}c)/L_P$; $\Lambda_P = 2$, $\Lambda_P = 3$.